# Wigner-Poisson Statistics of Topological Transitions in a Josephson Junction

C. W. J. Beenakker, J. M. Edge, J. P. Dahlhaus, D. I. Pikulin, Shuo Mi, and M. Wimmer

*Instituut-Lorentz, Universiteit Leiden, P.O. Box 9506, 2300 RA Leiden, The Netherlands*

(Received 14 May 2013; published 17 July 2013)

The phase-dependent bound states (Andreev levels) of a Josephson junction can cross at the Fermi level if the superconducting ground state switches between even and odd fermion parity. The level crossing is topologically protected, in the absence of time-reversal and spin-rotation symmetry, irrespective of whether the superconductor itself is topologically trivial or not. We develop a statistical theory of these topological transitions in an $N$-mode quantum-dot Josephson junction by associating the Andreev level crossings with the real eigenvalues of a random non-Hermitian matrix. The number of topological transitions in a $2\pi$ phase interval scales as $\sqrt{N}$, and their spacing distribution is a hybrid of the Wigner and Poisson distributions of random-matrix theory.

DOI: 10.1103/PhysRevLett.111.037001 PACS numbers: 74.45.+c, 03.65.Vf, 74.50.+r

The von Neumann–Wigner theorem of quantum mechanics forbids the crossing of two energy levels when a parameter is varied, unless the corresponding wave functions have a different symmetry [1]. One speaks of level repulsion. In disordered systems, typical for condensed matter, one would not expect any symmetry to survive and therefore no level crossing to appear. This is indeed the case in normal metals, but not in superconductors, where level crossings at the Fermi energy are allowed [2]. The symmetry that protects the level crossing is called fermion parity [3]: the parity of the number of electrons in the superconducting condensate switches between even and odd at a level crossing. To couple the two levels and open up a gap at the Fermi level, one would need to add or remove an electron from the condensate, which is forbidden in a closed system.

Fermion-parity switches in superconductors have been known since the 1970s [4,5], but recently they have come under intense investigation in connection with Majorana fermions and topological superconductivity [6–14]. A pair of Majorana zero modes appears at each level crossing, and the absence of level repulsion expresses the fact that two Majorana fermions represent one single state [2]. Topologically nontrivial superconductors are characterized by an odd number of level crossings when the superconducting phase is advanced by $2\pi$, resulting in a $4\pi$ periodicity of the Josephson effect [3,15].

Here we announce and explain an unexpected discovery: sequences of fermion-parity switches are not independent. As illustrated in Fig. 1, for a quantum-dot model Hamiltonian [16], the level crossings show an antibunching effect, with a spacing distribution that vanishes at small spacings. This is reminiscent of level repulsion, but we find that the spacing distribution is distinct from the Wigner distribution of random Hamiltonians [17,18]. Instead, it is a hybrid of the Wigner distribution (linear repulsion) for small spacings and the Poisson distribution (exponential tail) for large spacings. This Wigner-Poisson statistics has appeared once before in condensed matter physics at the Anderson metal-insulator transition [19,20]. We construct an ensemble of non-Hermitian matrices that describes the hybrid statistics, in excellent agreement with simulations of a microscopic model.

The geometry considered is shown in Fig. 2. It is an Andreev billiard [21]: a semiconductor quantum dot with chaotic potential scattering and Andreev reflection at superconductors $S_1$ and $S_2$. We distinguish two types of coupling to the superconductors: a strong local coupling by a ballistic point contact and a weak uniform coupling by a tunnel barrier. In Fig. 2(a), both superconductors are coupled by a ballistic point contact with $N$ propagating modes (counting spin). The chaotic scattering in the quantum dot (mean level spacing $\delta$) then does not mix electrons and holes on the time scale $\tau_A \simeq \hbar/N\delta$ between Andreev reflections at the point contacts. In Fig. 2(b), only $S_1$ is coupled locally. The uniform coupling to the other superconductor $S_2$ ensures that the entire phase space of electrons and holes is mixed chaotically within a time $\tau_A$. These two geometries correspond to different random-matrix ensembles, essentially two extreme cases, but we will see that the statistical results are very similar.

We need to break both spin-rotation and time-reversal symmetry (symmetry class D) to permit level crossings [2]. Spin-rotation symmetry is broken by spin-orbit coupling on a time small compared to $\tau_A$. Time-reversal symmetry is broken by a magnetic field $B$. A weak field is sufficient, one flux quantum $h/e$ through the quantum dot and negligible Zeeman energy, so we may assume that the spin-singlet $s$-wave pairing in $S_n$ remains unperturbed. One then has a topologically trivial superconductor without the unpaired Majorana fermions associated with a band inversion [22].

We choose a gauge where the order parameter $\Delta_0$ in $S_2$ is real, while $S_1$ is phase biased at $e^{i\phi}\Delta_0$. The excitation spectrum of this Josephson junction is discrete for $|E| < \Delta_0$ and $\pm E$ symmetric because of electron-hole symmetry. As $\phi$ is advanced by $2\pi$, pairs of excitation energies

 

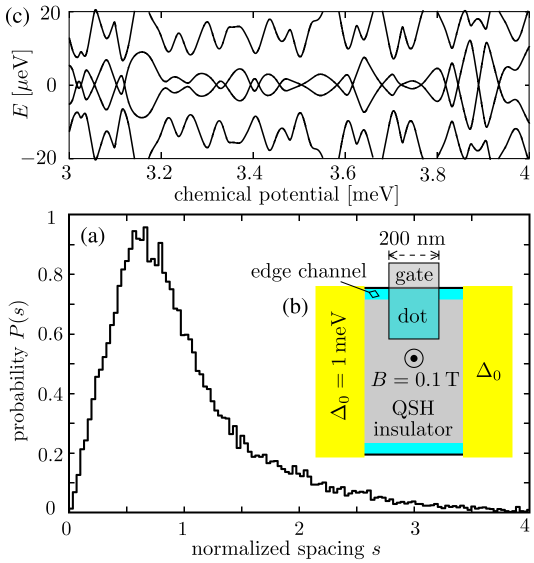


FIG. 1 (color online). Model calculation of level crossings for a quantum-dot Josephson junction in an InAs-GaSb quantum well (material parameters as in Ref. [16]). Panel (a) shows the spacing distribution sampled over disorder realizations for $\simeq 50$ level crossings in a 3–6 meV chemical potential interval. Panel (b) shows the geometry of the device; panel (c) shows the level crossings for a single sample.

$\pm E_n(\phi)$ may cross. The associated $\mathbb{Z}_2$ topological quantum number switches between $\pm 1$ at each level crossing [3], indicating a switch between an even and odd number of electrons in the ground state. At a constant total electron number, the switch in the ground-state fermion parity is accompanied by the filling or emptying of an excited state. We seek the statistics of these topological transitions.

The geometry of Fig. 2(b) is somewhat easier to analyze than Fig. 2(a), so we do that first. Electrons and holes $(e, h)$ at the Fermi level propagate through the point contact between $S_1$ and the quantum dot in one of the $N = 2M$ modes. (The factor of 2 accounts for the $\uparrow, \downarrow$ spin degree of freedom.) Left-moving quasiparticles are Andreev reflected by $S_1$ and right-moving quasiparticles are reflected by the quantum dot coupled to $S_2$. The vector $\Psi = (\Psi_{e\uparrow}, \Psi_{e\downarrow}, \Psi_{h\uparrow}, \Psi_{h\downarrow})$ of wave amplitudes is transformed as $\Psi \mapsto R_2 R_1 \Psi$ by multiplication with the reflection matrices

$$R_1(\phi) = \begin{pmatrix} 0 & e^{-i\phi}\Lambda \\ e^{i\phi}\Lambda^{\mathrm{T}} & 0 \end{pmatrix}, \qquad \Lambda = \bigoplus_{m=1}^{M} \begin{pmatrix} 0 & -i \\ i & 0 \end{pmatrix}, \tag{1}$$

$$R_2 = \begin{pmatrix} r_{ee} & r_{eh} \\ r_{he} & r_{hh} \end{pmatrix}, \qquad r_{hh} = r_{ee}^*, \qquad r_{eh} = r_{he}^*. \tag{2}$$

These are $2N \times 2N$ unitary matrices, with four $N \times N$ sub-blocks related by electron-hole symmetry. The sign of the determinant of the reflection matrix distinguishes topologically trivial from nontrivial superconductivity [23]. We take both superconductors $S_1$ and $S_2$ as being topologically trivial by fixing Det $R_n = 1$. (The topologically nontrivial case is considered later on.)

The condition for a level crossing at phase $\phi$ is that $\Psi$ is an eigenstate of $R_2 R_1(\phi)$ with a unit eigenvalue, so

$$\mathrm{Det}[1 - R_2 R_1(\phi)] = 0. \tag{3}$$

We seek to rewrite this as an eigenvalue equation for some real matrix $\mathcal{M}$. For that purpose, we change variables from phase $\phi \in (-\pi, \pi)$ to quasienergy $\varepsilon = \tan(\phi/2) \in (-\infty, \infty)$. Equation (3) then takes the form

$$\mathrm{Det}[1 - U - i\varepsilon(1 + U)\tau_z] = 0, \qquad \tau_z = \begin{pmatrix} 1 & 0 \\ 0 & -1 \end{pmatrix}, \tag{4}$$

with $U = R_2 R_1(0)$. The Pauli matrix $\tau_z$ acts on the electron-hole blocks, to be distinguished from the Pauli spin matrix $\sigma_z$.

The complex unitary matrix $U$ becomes a real orthogonal matrix $O$ upon a change of basis,

$$O = \Omega^\dagger U \Omega, \qquad \Omega = \frac{1}{\sqrt{2}} \begin{pmatrix} 1 & i \\ 1 & -i \end{pmatrix}. \tag{5}$$

Note that Det $O$ = Det $U = 1$, so $O \in \mathrm{SO}(2N)$ is special orthogonal. Since $\Omega^\dagger \tau_z \Omega = -\tau_y$, the level crossing condition becomes

$$\mathrm{Det}[1 - O + \varepsilon(1 + O)J] = 0, \qquad J = i\tau_y = \begin{pmatrix} 0 & 1 \\ -1 & 0 \end{pmatrix}. \tag{6}$$

For chaotic scattering, $O$ is uniformly distributed with the Haar measure of SO($2N$). This is the circular real ensemble (CRE) of random-matrix theory (RMT) in symmetry class D [2,24].

The special orthogonal matrix $O$ can be represented by an antisymmetric real matrix $A = -A^{\mathrm{T}}$ through the Cayley transform [25]

$$O = (1 - A)(1 + A)^{-1}. \tag{7}$$

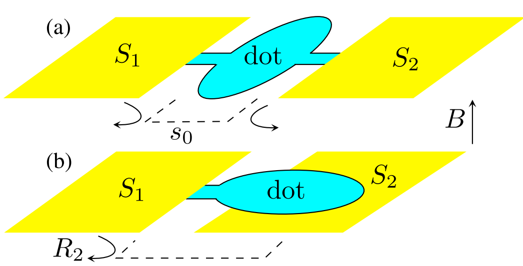


FIG. 2 (color online). Two designs of a quantum-dot Josephson junction. In (a) the quantum dot is coupled locally by point contacts to both superconductors $S_1$ and $S_2$, while in (b) coupling to $S_1$ is local while $S_2$ is coupled uniformly to the entire phase space of the quantum dot. In (a) the chaotic scattering refers only to the normal-state scattering matrix $s_0$, while in (b) the combined reflection from dot plus $S_2$ is described by a chaotic scattering matrix $R_2$.

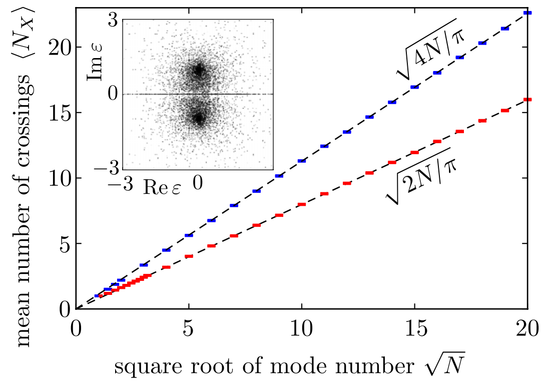


FIG. 3 (color online). Plot of the $N$ dependence of the average number $\langle N_X\rangle$ of distinct real eigenvalues $\varepsilon$ calculated for the skew-Hamiltonian ensemble constructed from a uniformly distributed $s_0 \in \mathrm{U}(2N)$ (lower set of red data points with a scatter plot for $N = 50$ in the inset) and $O \in \mathrm{SO}(2N)$ (upper set of blue data points). These are the expected number of level crossings (topological transitions) in a $2\pi$ phase interval for the quantum-dot Josephson junction in Figs. 2(a) (red) and 2(b) (blue). The analytical formulas given by the dashed lines have the status of a conjecture.

The substitution of Eq. (7) into Eq. (6) gives the level crossing condition as an eigenvalue equation,

$$\mathrm{Det}(\mathcal{M} - \varepsilon) = 0, \qquad \mathcal{M} = AJ = (1 - O)(1 + O)^{-1}J. \quad (8)$$

The matrix $\mathcal{M}$ is real but not symmetric: $\mathcal{M}^{\mathrm{T}} = -J\mathcal{M}J$. This is the definition of a skew-Hamiltonian matrix. There are $N$ distinct eigenvalues, each with multiplicity 2 [26]. The $N_X$ distinct real eigenvalues $\varepsilon_n$ identify the level crossings at $\phi_n = 2\arctan\varepsilon_n$.

We have thus transformed the level crossing problem into a classic problem of random-matrix theory [27–31]: how many eigenvalues of a real matrix are real? One might have guessed that an eigenvalue is exactly real with vanishing probability, since the real axis has measure zero in the complex plane. Instead, the eigenvalues of real non-Hermitian matrices accumulate on the real axis (see Fig. 3, inset). This accumulation is a consequence of the fact that the complex eigenvalues come in pairs $\varepsilon$, $\varepsilon^*$, so real eigenvalues are stable: they cannot be pushed into the complex plane by a weak perturbation.

The eigenvalue distribution is known exactly for independent normally distributed matrix elements (the Ginibre ensemble [32–35]). For large $N$, there are on average $\langle N_X\rangle \propto \sqrt{N}$ real eigenvalues [28]. The spacing distribution vanishes as $s^\beta$ for small spacings $s$ (normalized by the average spacing), with $\beta = 1$ on the real axis (linear level repulsion) [27,29]. These power laws are derived for uncorrelated matrix elements, but we find numerically [36] that both the $\sqrt{N}$ scaling (Fig. 3) and the linear repulsion (Fig. 4) hold for our ensemble of skew-Hamiltonian matrices.

The linear repulsion for $s \lesssim 1$ crosses over into an exponential tail for $s \gtrsim 1$. As one can see in Fig. 4, the semi-Poisson distribution [19,20,38,39] interpolates quite

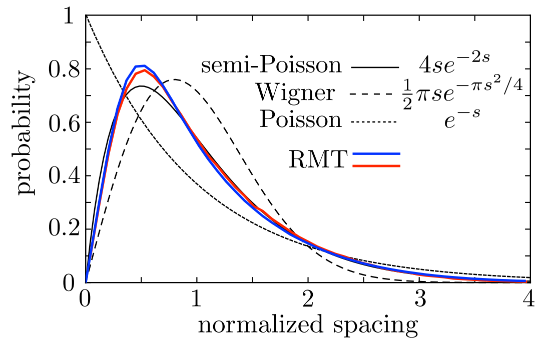


FIG. 4 (color online). Probability distribution of the normalized spacings $s = \delta\phi/\langle\delta\phi\rangle$ of level crossings calculated for the random-matrix ensemble of Figs. 2(a) (red curve) and 2(b) (blue), with $N = 100$. The distributions are obtained by generating a large number of matrices and separating them in sets having the same number $N_X$ of real eigenvalues $\varepsilon = \tan(\phi/2)$, with average spacing $\langle\delta\phi\rangle = 2\pi/N_X$. A weighted average $P(s) = \sum_{N_X} P(s|N_X)P(N_X)$ of the spacing distribution within each set is plotted in the figure. The black curves show three analytical spacing distributions.

accurately between these small- and large-$s$ limits and describes the numerical random-matrix theory results better than either the Poisson distribution of uncorrelated eigenvalues or the Wigner surmise of the Gaussian orthogonal ensemble [17,18].

The same power laws apply to topologically nontrivial superconductors. We then need reflection matrices $R_1$, $R_2$ with determinant $-1$, which can be achieved by assuming that a sufficiently large Zeeman energy allows for an unpaired spin channel, and adding this channel as a unit diagonal element to $\Lambda = \mathrm{diag}(1, \sigma_y, \sigma_y \ldots \sigma_y)$. The determinant of the product $R_1R_2$ remains equal to $+1$, so $O \in \mathrm{SO}(2N)$ remains special orthogonal, with $N = 2M + 1$ an odd rather than even integer. Since the eigenvalues of $\mathcal{M}$ come in complex conjugate pairs, the number $N_X$ of distinct real eigenvalues (and hence the number of level crossings) is now also odd rather than even. This even or odd difference does not affect either the $\sqrt{N}$ scaling or the linear repulsion.

So far we considered the geometry of Fig. 2(b) with a chaotic mixing of electron and hole degrees of freedom in the quantum dot. In Fig. 2(a) the quantum dot does not couple electrons and holes, so the random-matrix ensemble is different. The chaotic scattering of electrons in the quantum dot is then described by $N \times N$ reflection and transmission matrices, which together form the unitary scattering matrix $s_0$. The scattering matrix for holes at the Fermi level is just the complex conjugate $s_0^*$. Instead of the CRE, we now have the circular unitary ensemble [40] corresponding to a uniform distribution of $s_0 \in \mathrm{U}(2N)$ with the Haar measure of the unitary group. We again find a $\sqrt{N}$ scaling of the number of transitions and a hybrid Wigner-Poisson spacing distribution (red lines in Figs. 3 and 4) [41].

To test these model-independent results of RMT, we have performed computer simulations of two microscopic models, one topologically trivial and the other nontrivial. The first model is that of an InSb Josephson junction, similar to that studied in a recent experimental search for Majorana fermions [42]. One crucial difference is that we take a weak perpendicular magnetic field, just a few flux quanta $h/e$ through the junction that is sufficient to break time-reversal symmetry but not strong enough to induce a transition to a topologically nontrivial state (which would require Zeeman energy comparable to a superconducting gap [22]).

The model Hamiltonian has the Bogoliubov–de Gennes form,

$$\mathcal{H} = \begin{pmatrix} H_0(\boldsymbol{p} - e\boldsymbol{A}) & \Delta \\ \Delta^* & -\sigma_y H_0^*(-\boldsymbol{p} - e\boldsymbol{A})\sigma_y \end{pmatrix},$$

$$H_0(\boldsymbol{p}) = \frac{1}{2}p^2/m_{\rm eff} + U - E_{\rm F} + \hbar^{-1}\alpha_{\rm so}(\sigma_x p_y - \sigma_y p_x), \quad (9)$$

with electron and hole blocks coupled by the $s$-wave pair potential $\Delta$ at the superconducting contacts. The single-particle Hamiltonian $H_0$ contains the Rasba spin-orbit coupling of an InSb quantum well (characteristic length $l_{\rm so} = \hbar^2/m_{\rm eff}\alpha_{\rm so} = 0.25\ \mu$m) and an electrostatic disorder potential $U$. The vector potential $\boldsymbol{A} = (0, Bx, 0)$ accounts for the orbital effect of a perpendicular magnetic field $B$ (which we set equal to zero in the superconductors). The Zeeman term has a negligible effect and is omitted. The Fermi energy $E_{\rm F}$ is chosen such that the InSb channel has $N = 20$ transverse modes at the Fermi level, including spin. We discretize the model on a two-dimensional square lattice, with disorder potential $U \in (-U_0, U_0)$ chosen randomly and independently on each site. The low-lying energy levels of the resulting tight-binding Hamiltonian are computed [43] as a function of the phase difference $\phi$ of the pair potential.

In Fig. 5 we compare the results of the InSb model calculation [44] with the RMT predictions in the quantum-dot geometry of Fig. 2(a). The disordered InSb channel lacks the point contact coupling of a quantum dot, so the scattering is not fully chaotic and no precise agreement with the RMT calculations is to be expected. Indeed, the probabilities $P(N_X)$ to have $N_X$ level crossings for $N = 20$ modes shown in Fig. 5(d) agree only qualitatively. Still, the spacing distributions shown in Fig. 5(a) for $N_X = 4$ are in remarkable agreement without any adjustable parameter.

The second microscopic model that we have studied is topologically nontrivial: the quantum spin-Hall (QSH) insulator in a InAs/GaSb quantum well [45,46]. The Hamiltonian still has the Bogoliubov–de Gennes form (9), but now $H_0$ is the four-band Bernevig-Hughes-Zhang Hamiltonian [47]. The quantum dot is formed using the method of Ref. [16] by locally pushing the conduction band below the Fermi level by means of a gate electrode. The QSH insulator has a single conducting mode at the edge

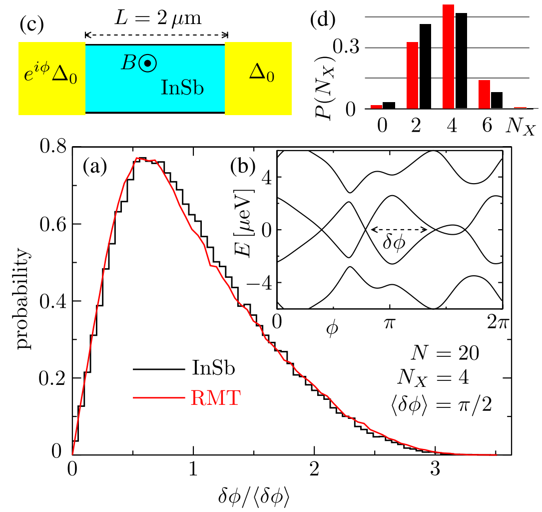


FIG. 5 (color online). Panel (a): spacing distribution of $N_X = 4$ level crossings in a Josephson junction with $N = 20$ transverse modes. The red curve shows the RMT prediction in the geometry of Fig. 2(a). The black histogram is a model calculation [44] for a disordered InSb channel in a perpendicular magnetic field sampled over different impurity configurations [the inset (b) shows level crossings for one sample and panel (c) shows the geometry]. Panel (d) compares the probability of $N_X$ level crossings for $N = 20$ in the RMT calculation (red curve) and in the InSb model (black).

[48,49], so $N = 1$ and our large-$N$ RMT is not directly applicable. Still, as shown in Fig. 1, a linear repulsion at small spacings still applies if we count the level crossings as a function of the chemical potential in the quantum dot—demonstrating the universality of this effect.

In conclusion, we have discovered a statistical correlation in the fermion-parity switches of a Josephson junction. The spacing distribution of these topological phase transitions has a universal form—a hybrid of the Wigner and Poisson distributions—decaying linearly at small spacings and exponentially at large spacings. Such a hybrid (semi-Poisson or "mermaid") distribution is known from Anderson phase transitions [19,20], where it signals a fractal structure of wave functions. It would be interesting for further theoretical work to investigate whether this self-similar structure appears here as well. Experimentally, it would be of interest to search for the repulsion of level crossings by tunnel spectroscopy [12].

We thank A. R. Akhmerov for discussions and help with the random-matrix calculations. This work was supported by the Dutch Science Foundation NWO/FOM, by an ERC Advanced Investigator Grant, by the EU network NanoCTM, and by the China Scholarship Council.

[1] J. von Neumann and E. Wigner, Phys. Z. **30**, 467 (1929).
[2] A. Altland and M. R. Zirnbauer, Phys. Rev. B **55**, 1142 (1997).

[3] A. Yu. Kitaev, Phys. Usp. **44** (Supplement), 131 (2001).
[4] A. Sakurai, Prog. Theor. Phys. **44**, 1472 (1970).
[5] A. V. Balatsky, I. Vekhter, and J.-X. Zhu, Rev. Mod. Phys. **78**, 373 (2006).
[6] S. Ryu, A. Schnyder, A. Furusaki, and A. Ludwig, New J. Phys. **12**, 065010 (2010).
[7] B. M. Andersen, K. Flensberg, V. Koerting, and J. Paaske, Phys. Rev. Lett. **107**, 256802 (2011).
[8] K. T. Law and P. A. Lee, Phys. Rev. B **84**, 081304 (2011).
[9] C. W. J. Beenakker, D. I. Pikulin, T. Hyart, H. Schomerus, and J. P. Dahlhaus, Phys. Rev. Lett. **110**, 017003 (2013).
[10] T. Yokoyama, M. Eto, and Yu. V. Nazarov, J. Phys. Soc. Jpn. **82**, 054703 (2013).
[11] E. J. H. Lee, X. Jiang, R. Aguado, G. Katsaros, C. M. Lieber, and S. De Franceschi, Phys. Rev. Lett. **109**, 186802 (2012); E. J. H. Lee *et al.*, arXiv:1302.2611.
[12] W. Chang, V. E. Manucharyan, T. S. Jespersen, J. Nygård, and C. M. Marcus, Phys. Rev. Lett. **110**, 217005 (2013).
[13] J. D. Sau and E. Demler, arXiv:1204.2537.
[14] R. Ilan, J. H. Bardarson, H.-S. Sim, and J. E. Moore, arXiv:1305.2210.
[15] H.-J. Kwon, K. Sengupta, and V. M. Yakovenko, Eur. Phys. J. B **37**, 349 (2004).
[16] S. Mi, D. I. Pikulin, M. Wimmer, and C. W. J. Beenakker, Phys. Rev. B **87**, 241405(R) (2013).
[17] M. L. Mehta, *Random Matrices* (Elsevier, New York, 2004).
[18] P. J. Forrester, *Log-Gases and Random Matrices* (Princeton University Press, Princeton, NJ, 2010).
[19] B. I. Shklovskii, B. Shapiro, B. R. Sears, P. Lambrianides, and H. B. Shore, Phys. Rev. B **47**, 11487 (1993).
[20] E. B. Bogomolny, U. Gerland, and C. Schmit, Phys. Rev. E **59**, R1315 (1999).
[21] C. W. J. Beenakker, Lect. Notes Phys. **667**, 131 (2005).
[22] J. Alicea, Rep. Prog. Phys. **75**, 076501 (2012).
[23] A. R. Akhmerov, J. P. Dahlhaus, F. Hassler, M. Wimmer, and C. W. J. Beenakker, Phys. Rev. Lett. **106**, 057001 (2011).
[24] C. W. J. Beenakker, J. P. Dahlhaus, M. Wimmer, and A. R. Akhmerov, Phys. Rev. B **83**, 085413 (2011).
[25] The Cayley transform (7) does not exist if Det $O = -1$, which happens if one superconductor is topologically trivial and the other nontrivial. Then the quantum dot contains an unpaired Majorana zero mode at any value of $\phi$, so the whole notion of level crossings loses its meaning.
[26] The twofold degeneracy of the eigenvalues of a skew-Hamiltonian matrix follows directly from the fact that the determinant (8) can equivalently be written as the square of a Pfaffian: $[\mathrm{Pf}(A + \varepsilon J)]^2 = 0$. The sign of this Pfaffian is the topological quantum number representing the ground-state fermion parity.
[27] N. Lehmann and H.-J. Sommers, Phys. Rev. Lett. **67**, 941 (1991).
[28] A. Edelman, E. Kostlan, and M. Shub, J. Am. Math. Soc. **7**, 247 (1994); A. Edelman, J. Multivariate Anal. **60**, 203 (1997).
[29] E. Kanzieper and G. Akemann, Phys. Rev. Lett. **95**, 230201 (2005).
[30] P. J. Forrester and T. Nagao, Phys. Rev. Lett. **99**, 050603 (2007).
[31] B. A. Khoruzhenko and H.-J. Sommers, in *Handbook on Random Matrix Theory*, edited by G. Akemann, J. Baik, and P. Di Francesco (Oxford University Press, Oxford, 2011).
[32] J. Ginibre, J. Math. Phys. (N.Y.) **6**, 440 (1965).
[33] V. L. Girko, Theory Probab. Appl. **29**, 694 (1985).
[34] T. Tao and V. Vu, Ann. Probab. **38**, 2023 (2010).
[35] C. Bordenave and D. Chafaï, Probab. Surv. **9**, 1 (2012).
[36] Random unitary and orthogonal matrices were generated using the method of F. Mezzadri, Not. Am. Math. Soc. **54**, 592 (2007); eigenvalues of skew-Hamiltonian matrices were calculated using the algorithm of P. Benner, D. Kressner, and V. Mehrmann, in *Proceedings of the Conference on Applied Mathematics and Scientific Computing* (Springer, Amsterdam, 2005). For details of these random-matrix calculations, see [37].
[37] See Supplemental Material at http://link.aps.org/supplemental/10.1103/PhysRevLett.111.037001 for the random-matrix calculations.
[38] T. Gorin, M. Müller, and P. Seba, Phys. Rev. E **63**, 068201 (2001).
[39] A. M. García-García and J. Wang, Phys. Rev. E **73**, 036210 (2006).
[40] F. J. Dyson, J. Math. Phys. (N.Y.) **3**, 140 (1962).
[41] We have found that the same hybrid Wigner-Poisson spacing distribution of real eigenvalues applies also to the Ginibre ensemble, see the Supplemental Material [37].
[42] L. P. Rokhinson, X. Liu, and J. K. Furdyna, Nat. Phys. **8**, 795 (2012).
[43] The tight-binding model calculations were performed using the KWANT package developed by A. R. Akhmerov, C. W. Groth, X. Waintal, and M. Wimmer, http://www.kwant-project.org; to efficiently calculate the lowest energy levels, we used the ARPACK package developed by R. Lehoucq, K. Maschhoff, D. Sorensen, and C. Yang, http://www.caam.rice.edu/software/ARPACK.
[44] Parameters used for the InSb model calculation in Fig. 5 are magnetic field $B = 6.2$ mT corresponding to a flux $3h/e$ through an area $L \times W = 2\ \mu\mathrm{m} \times 1\ \mu\mathrm{m}$, spin-orbit length $l_{\mathrm{so}} = 0.25\ \mu\mathrm{m}$, lattice constant $a = l_{\mathrm{so}}/10$, Fermi energy $E_{\mathrm{F}} = 2.5$ meV corresponding to $N = 20$ transverse modes, superconducting gap $\Delta_0 = 0.4$ meV, and disorder strength $U_0 = 1.7$ meV corresponding to a mean free path $l \approx L/2$.
[45] C. Liu, T. L. Hughes, X.-L. Qi, K. Wang, and S.-C. Zhang, Phys. Rev. Lett. **100**, 236601 (2008).
[46] I. Knez, R.-R. Du, and G. Sullivan, Phys. Rev. Lett. **107**, 136603 (2011); **109**, 186603 (2012).
[47] B. A. Bernevig, T. L. Hughes, and S. C. Zhang, Science **314**, 1757 (2006).
[48] M. Z. Hasan and C. L. Kane, Rev. Mod. Phys. **82**, 3045 (2010).
[49] X.-L. Qi and S.-C. Zhang, Rev. Mod. Phys. **83**, 1057 (2011).